AGH Journal of Mining and Geoengineering • vol. 36 • No. 3 • 2012

*Yucang Wang**, *Sheng Xue**, *Jun Xie**

A FULLY COUPLED SOLID AND FLUID MODEL FOR SIMULATING COAL AND GAS OUTBURST WITH DEM AND LBM

1. Introduction

A fundamental challenge to effectively predict and control the outburst is to understand its physical mechanism and factors contributing to its initiation and development. Field observations and laboratory studies reveal that the occurrence of the outburst is the result of combined effects of stress redistribution, gas desorption, coal property and time effects [1–4]. The use of numerical simulations can provide useful insights on outbursts. Along this line, there are already some attempts [5–11]. However these models do not model solid fracture and fragmentation explicitly. Free flow of fluid and two-way interactions between the solid and fluid are also missing.

In this study, a new outburst model which includes the most recognized effecting factors of outbursts is presented. The model couples two well developed numerical approaches: the Discrete Element Method (DEM) and the Lattice Boltzmann Method (LBM).

2. Model

The DEM is a powerful numerical tool and has been extensively used in many scientific and engineering problems [12]. The Esys_Particle code, an open source DEM code, is used in this study. Detailed information about the model and the code can be found in open literature [13–17].

* CSIRO Earth Science and Resource Engineering, P.O. Box 833, Kenmore, QLD 4069, Brisbane, Australia

In recent years, the LBM has made brilliant progress as a new method in numerical modeling of fluid dynamics. The LBM solves the particle distribution function *f*. The completely discretized equation, with the time step Δt and space step Δx, is given by BGK model [18].

$$f_\alpha\left(x_i + e_\alpha, t + \Delta t\right) - f_\alpha\left(x_i, t\right) = -\frac{1}{\tau}\left[f_\alpha\left(x_i, t\right) - f_\alpha^{eq}\left(x_i, t\right)\right] \tag{1}$$

where:

τ — denotes the lattice relaxation time,
e_α — is the discrete lattice velocity in direction,
α, x_i — is a point in the discretized physical space,
f_α^{eq} — is the equilibrium distribution function.

Eq. (1) is usually solved in the following two steps: collision and streaming step:

$$\tilde{f}_\alpha\left(x_i, t + \Delta t\right) - f_\alpha\left(x_i, t\right) = -\frac{1}{\tau}\left[f_\alpha\left(x_i, t\right) - f_\alpha^{eq}\left(x_i, t\right)\right] \tag{2}$$

$$f_\alpha\left(x_i + e_\alpha, t + \Delta t\right) = \tilde{f}_\alpha\left(x_i, t + \Delta t\right) \tag{3}$$

where $\tilde{f}_\alpha$ — represents the post-collision state.

In this study, the open source code, OpenLB [19], is used to couple with the Esys_Particle code. There are several issues to be addressed for such coupling: moving boundary conditions for a curved shape; momentum transfer between solid particle and fluid; and force from fluid to solid particles.

The particle surface can intersect the link between two nodes at arbitrary distance with a ratio of $\delta = \left|x_f - x_w\right| / \left|x_f - x_b\right|$ (Fig. 1). The reflected distribution function at node x_f can be calculated using an interpolation scheme [20]

$$\begin{aligned} f_{\tilde{\alpha}}\left(x_f, t + \Delta t\right) = \frac{1}{1+\delta}\Big[&(1-\delta)\cdot f_\alpha\left(x_f, t + \Delta t\right) + \delta \cdot f_\alpha\left(x_b, t + \Delta t\right) \\ &+ \delta \cdot f_{\tilde{\alpha}}\left(x_{f2}, t + \Delta t\right) - 6 w_\alpha \rho_w e_\alpha \cdot u_w / c^2\Big] \end{aligned} \tag{4}$$

where:

w_α — is the weight factor,
ρ_w — is the fluid density at node x_f (Fig. 1),
u_w — is the velocity of the solid particle.

The fluid force acted on the particle surface can be obtained using

$$F = \sum_{x_b} \sum_{\alpha=1}^{9} e_\alpha \left[f_\alpha \left(x_b, t \right) + f_{\bar{\alpha}} \left(x_f, t + \Delta t \right) \right] \Delta x / \Delta t \tag{5}$$

where the first summation is taken over all fluid nodes at x_b adjacent to the particle and the second is taken over all possible lattice directions pointing towards a particle cell. This force is added to the particle force in DEM code.

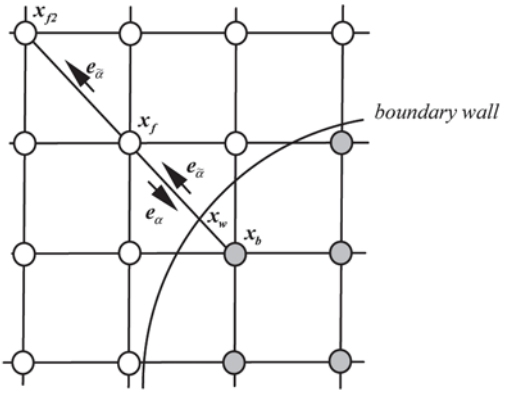

Fig. 1. The moving curved wall boundary condition

Darcy flow is modeled by LBM code by considering the translational collision step as a second intermediate step after streaming, denoted by f^{**}

$$f_\alpha^{**} \left(x, t + \Delta t \right) = f_\alpha^{*} \left(x, t \right) - \frac{1}{\tau} \left[f^{*}{}_\alpha \left(x, t \right) - f_\alpha^{eq} \left(x, t \right) \right] \tag{7}$$

Then the porous medium step has the form

$$f_\alpha \left(x, t + \Delta t \right) = f_\alpha^{**} \left(x, t + \Delta t \right) + n_s \left[f_{\bar{\alpha}}^{**} \left(x + e_\alpha, t + \Delta t \right) - f_\alpha^{**} \left(x, t + \Delta t \right) \right] \tag{8}$$

where n_s is a damping parameter introduced by Dardis and McCloskey [21–22]. Diffusion is managed by DEM part in the coupled scheme. It is assumed that there is an average and uniform pore pressure p_i and concentration c_i for each particle i.

The fluid exchange between two contacted particles *i* and *j* is determined by the Fick's first law of diffusion

$$\Delta V_f = D\left(c_i - c_j\right)\Delta t,$$

where D is the diffusion coefficient of the link.

The hydro-mechanical coupling can be implemented based on the Biot's linear pore-elastic theory [23]

$$\varepsilon = -\left(P - \alpha p\right)/K_m \tag{9}$$

$$\varsigma = -\alpha\left(P - p/B\right)/K_m \tag{10}$$

where:

p — is pore pressure,

$P = -\sigma_{kk}/3$ — is the mean or total mechanical pressure (isotropic compressive stress),

$\varepsilon = \varepsilon_{kk} = \dfrac{\Delta V}{V}$ — is the volumetric strain (positive for extension),

$\varsigma = V_f/V$ — is the variation of fluid content (positive corresponds to a "gain" fluid),

α — is Biot coefficient,

B — is the Skempton pore pressure coefficient,

K_m — is the drained bulk modulus of the material,

V and V_f — are the volume of the material and fluid respectively.

Desorption is implemented in both DEM and LBM codes. The reduction of concentration in a solid particle is described by

$$\frac{\partial c}{\partial t} = -\frac{1}{\tau_d}\left[c - c(p)\right] \tag{11}$$

where:

c — is average matrix gas concentration,

p — is gas pressure (Eq. 9),

τ_d — is sorption time,

$$c(p) = V_c / V$$

where:

V — is the volume of the particle,

V_c — the volume of adsorbed gas in the coal matrix at pressure p is described by the Langmuir adsorption isotherms:

$$V_c = \frac{pV_L}{P_L + p} \tag{12}$$

where V_L and P_L — are Langmuir volume and Langmuir pressure.

3. Preliminary results

Some preliminary numerical results are presented here. Figure 2 shows particle motion in the fluid. Three particles bonded as a rigid body are driven by the fluid flow (Poiseuille flow). The motion and rotation of the rigid body, as well as vortex behind it, are clearly observed. This example verifies the algorithm of the two-way coupling of solid and fluid: moving boundary condition and dragging forces.

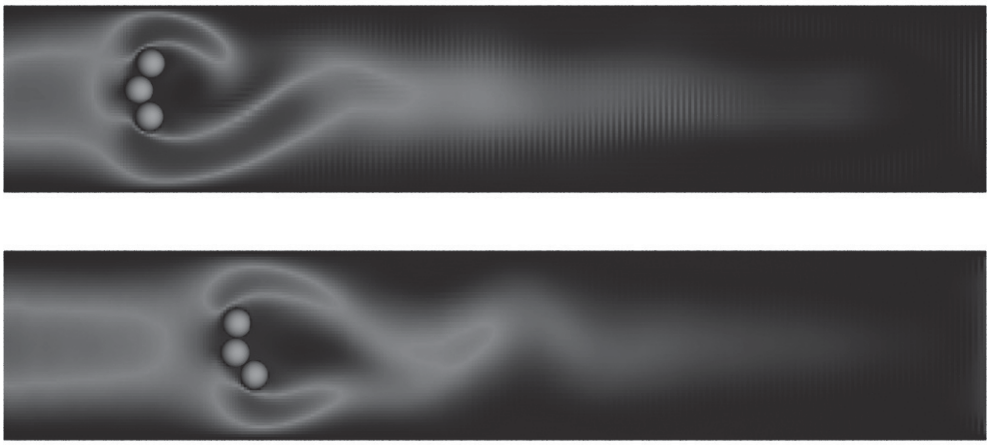

Fig. 2. Three bonded particle driving by fluid flow

A small outburst simulation is carried out. The model consists of 1003 equal-sized particles and 305×300 fluid grids. Constant confining pressures are applied at left, right, top and

bottom boundaries. The soft and fragile middle part (shown in dark and light grey in Figure 3), sandwiched by a harder and stronger rock, models a coal seam. Excavation starts from left side with constant speed by removing the dark grey part. Two supporting walls (horizontally dashed lines) are placed after the excavation, growing and following the moving excavation wall (vertical dashed line) at the right end (Fig. 3).

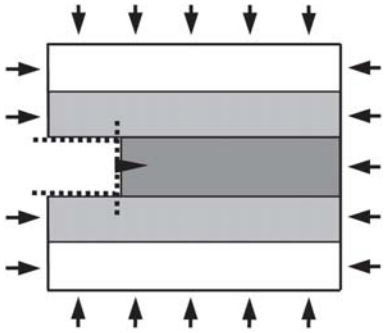

Fig. 3. Schematic diagram
of excavation and outburst simulation

Figure 4 shows the results of particle motion and fluid velocity at several time steps. In the early stage of excavation, there is no fracture events, and desorption of gas from the exposed surface is clearly observed. At the time step of 7000 (Fig. 4a) fractures occur at the excavation surface and excavation stops. After this the whole system of particle and fluid evolves by itself (Fig. 4b), and eventually the fractured coals are ejected from the face under exertion force of fluid and a cave with a small mouth and big inside void is formed, which is widely observed after the occurrence of an outburst in coal mines.

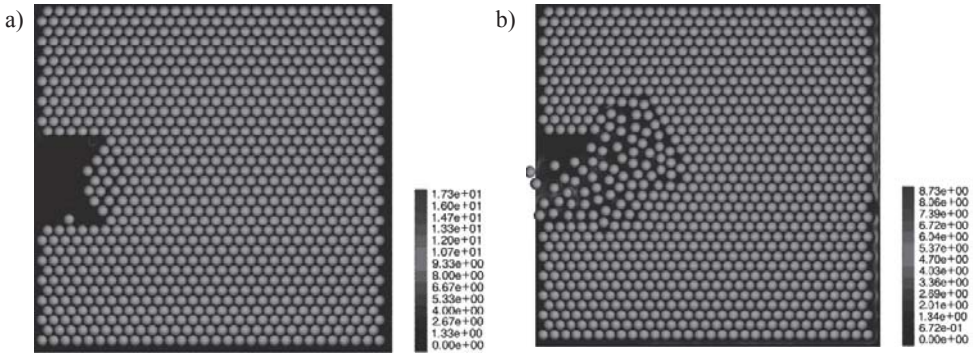

Fig. 4. Particle motion and fluid velocity during the outburst development:
a) time step = 4000; b) time step = 18400

Figure 5 shows the concentration of gas adsorbed in the solid coal at the same time steps with Figure 4. Lower concentration at the surface is observed due to desorption (Fig. 5a). The concentration changes in the inner particles are caused by diffusion process. The particles from the bursted coal have the lowest gas concentration (Fig. 5b) because they are totally exposed and have larger surface areas, therefore continue gas desorption while moving away from the face.

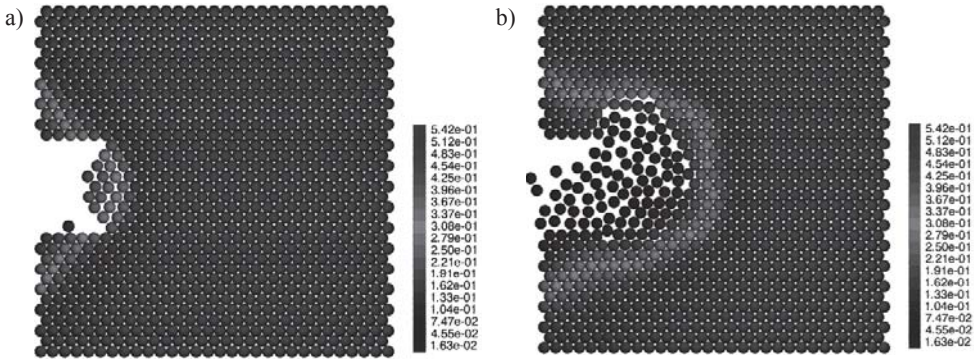

Fig. 5. Gas concentration at different time steps

It is observed that lower initial gas concentration will delay outbursts when all other parameters remain the same. This clearly suggests the important role of initial gas content played in outbursts. The sensitivity of outburst occurrence to other parameters will be further studied.

4. Summary

A new outburst model includes the most recognized factors of outbursts, including deformation, fracture and fragmentation of solids, free flow of fluid, Darcy flow, diffusion, desorption of gas, and two-way coupling of solid and fluid. The preliminary results with small scale simulations are encouraging as the whole outburst process is well reproduced. Current paper only presents the 2-D model. The 3-D model is under development. Although the input parameters are not calibrated to the practical data, and only small scale simulations are carried out currently, the new model has potential to numerically investigate the full mechanism and interaction of contributing factors of outburst.

REFERENCES

[1] *Lama R.D., Bodziony J.*: Management of outburst in underground coal mines, International Journal of Coal Geology 35: 83–115, 1998.

[2] *Cao Y.X., Davis A., Liu R.X., Liu X.W., Zhang Y.G.*: The influence of tectonic deformation on some geochemical properties of coals — a possible indicator of outburst potential, International Journal of Coal Geology 53: 69–79, 2003.

[3] *Li H.*: Major and minor structural features of a bedding shear zone along a coal seam and related gas outburst, Pingdingshan coalfield, northern China, International Journal of Coal Geology 35: 83–115, 2001.

[4] *Aguado M.B.D., Nicieza C.G.*: Control and prevention of gas outbursts in coal mines, Riosa-Olloniego coalfield, Spain, International Journal of Coal Geology 69: 253–266, 2007.

[5] *Litwiniszyn J.*: A model for initiation of gas outburst, International Journal of Rock Mechanics, Mining Sciences Geomechanics Abstract 22: 39–46, 1985.

[6] *Paterson L.*: A model for outbursts in coal. International Journal of Rock Mechanics Mining Sciences Geomechanics Abstract 23: 327–332, 1986.

[7] *Barron K., Kullmann D.*: Modeling of outburst at #26 Colliery, Glace Bay, Nova Scotia, Part 2, proposed outburst mechanism and model, Mining Science and Technology 2: 261–268, 1990.

[8] *Otuonye F., Sheng J.*: A numerical simulation of gas flow during coal/gas outbursts, Geotechnical and Geological Engineering 12: 15–34, 1994.

[9] Odintsev V.N.: Sudden outburst of coal and gas — failure of natural coal as a solution of methane in a solid substance, Journal of Mining Science 33: 508–516, 1997.

[10] *Xu T., Tang C.A., Yang T.H., Zhu W.C., Liu J.*: Numerical investigation of coal and gas outbursts in underground collieries, International Journal of Rock Mechanics Mining Sciences 43: 905–919, 2006.

[11] *Xue S., Wang Y.C., Xie J., Wang G.*: A coupled approach to simulate initiation of outbursts of coal and gas — model development, Int J Coal Geol 86: 222–230, 2011.

[12] *Cundall P.A., Strack O.*: A discrete element model for granular assemblies, Geotechnique 29: 47–65, 1979.

[13] *Mora P., Place D.*: A lattice solid model for the nonlinear dynamics of earthquakes, Int J Mod Phys C4: 1059–1074, 1993.

[14] *Wang Y.C.*: A new algorithm to model the dynamics of 3-D bonded rigid bodies with rotations, Acta Geotechnica 4: 117–127, 2009.

[15] *Wang Y.C., Mora P.*: Esys_Particle: A new 3-D discrete element model with single particle rotation. Advances in Geocomputing, Xing, H.L. (ed.), Springer, 183–288, 2009.

[16] *Wang Y.C., Alonso-Marroquin F.*: A finite deformation method for discrete element modeling: particle rotation and parameter calibration, Granular Matter 11: 331–343, 2009.

[17] https://launchpad.net/esys-particle.

[18] *Chen S., Doolen G.*: Lattice Boltzmann method for fluid flows, Anu Rev Fluid Mech 30: 329–364, 1998.

[19] http://www.numhpc.org/openlb/.

[20] *Yu D., Mei R., Luo L., Shyy W.*: Viscous flow computations with the method of lattice Boltzmann equation, Prog. Aerospace Sci 39: 329–367, 2003.

[21] *Dardis O., McClosky J.*: Permeability porosity relationships from numerical simulations of fluid flow, Geophys Res Lett 25: 1471–1474, 1998.

[22] *Dardis O., McClosky J.*: Lattice Boltzmann scheme with real numbered solid density for the simulation of flow in porous media, Phys Rev E 57: 4834–4837, 1998.

[23] *Detournay E., Cheng A.H.D.*: Fundamentals of poroelasticity, Comprehensive Rock Engineering: Principles, Practice and Projects, Vol. II, Analysis and Design Method, Pergamon Press, 1993.